Cell Biology International 33 (2009) 918–925

Cell Biology International

www.elsevier.com/locate/cellbi

2′-Epi-2′-*O*-acetylthevetin B induces apoptosis partly via Ca^{2+}-mediated mitochondrial pathway in human hepatocellular carcinoma HepG2 cells

Bo Feng [a], Cai-Guo Huang [a,*], Ruo-Hua Chen [c], Yue-Wei Guo [b], Bing-Hua Jiao [a,*]

[a] *Department of Biochemistry and Molecular Biology, Second Military Medical University, 800 Xiangyin Road, Shanghai 200433, People's Republic of China*
[b] *State Key Laboratory of Drug Research, Shanghai Institute of Materia Medica, Chinese Academy of Sciences, Shanghai 201203, People's Republic of China*
[c] *Changhai Hospital, Shanghai 200433, People's Republic of China*

Received 27 February 2009; revised 2 April 2009; accepted 3 June 2009

Abstract

2′-Epi-2′-*O*-acetylthevetin B (GHSC-74), a cardiac glycoside, can be isolated from the seeds of *Cerbera manghas* L. We demonstrated that GHSC-74 reduced the viability of HepG2 cells in a time- and dose-dependent manner, and efficiently induced apoptosis without significantly decreasing the viability of Chang human liver cells and Swiss albino 3T3 fibroblasts, as indicated by annexin-V/PI binding assay and Hoechst 33342 staining. In addition, stimulation of HepG2 cells with GHSC-74 induced a series of intracellular events: (1) loss of mitochondrial membrane potential; (2) sustained elevation of cytosolic [Ca^{2+}]; and (3) downregulation of Bcl-2. BAPTA-AM, a cytosolic Ca^{2+} chelator, partly suppressed cell death and prevented mitochondrial membrane potential from losing in GHSC-74-treated HepG2 cells. In contrast, EGTA, an extracellular Ca^{2+} chelator, exhibited a weaker effect as compared to that of BAPTA-AM. Taken together, the Ca^{2+}-mediated mitochondrial pathway was found to be involved in GHSC-74-induced HepG2 cell apoptosis.

Keywords: 2′-Epi-2′-*O*-acetylthevetin B(GHSC-74); Apoptosis; Ca^{2+}; Mitochondrial membrane potential ($\Delta\Psi m$); HepG2; Bcl-2

1. Introduction

2′-Epi-2′-O-acetylthevetin B (GHSC-74; Fig. 1) has been isolated from the seeds of *Cerbera manghas* L (Abe and Yamauchi, 1977), which belongs to the class of steroid-like compounds called cardiac glycosides. Their continued efficacy in the treatment of congestive heart failure and dysrhythmia is well known (Altamirano et al., 2006; Braunwald, 1985). However, there is little knowledge about the role of these compounds in the prevention and/or treatment of proliferative diseases such as cancer. In the last 5 years, these compounds have been shown to be involved in complex cell-signal transduction mechanisms, inducing selective control of human tumors rather than normal cellular proliferation (Wilhelm and Georgios, 2007; Steffen et al., 2006), and as such represent a promising candidate for targeted cancer chemotherapy.

Hepatic resection and liver transplantation are the two mainstays of curative treatment for hepatocellular carcinoma (HCC), but can only be applied to the early stage of HCC (Poon et al., 2001; Schwartz, 2004). The majority of patients with HCC are diagnosed at a late stage when curative treatment is not applicable. Thus, developing new therapeutic and preventive strategies inducing apoptosis could be effective in controlling the proliferation and invasiveness, having found a prognosis of advanced stage HCC.

Ca^{2+} is one of the most versatile universal signaling mediators of cellular apoptosis. Several findings indicate that mitochondrial Ca^{2+} accumulation plays a central and intrinsic role in mediating cellular apoptosis (Nutt et al., 2002; Orrenius, 2004; Scorrano et al., 2001). Although the importance of the endoplasmic reticulum (ER) as the major storage organelle is indisputable, studies have demonstrated that mitochondrial sequestration of large amounts of Ca^{2+} contributed to cell

* Corresponding authors. Tel.: +86 21 81870970 8020; fax: +86 21 65334344.
E-mail addresses: huangcaiguo@hotmail.com (C.-G. Huang), jiaobh@uninet.com.cn (B.-H. Jiao).

1065-6995/$ - see front matter © 2009 International Federation for Cell Biology. Published by Elsevier Ltd. All rights reserved.
doi:10.1016/j.cellbi.2009.06.013

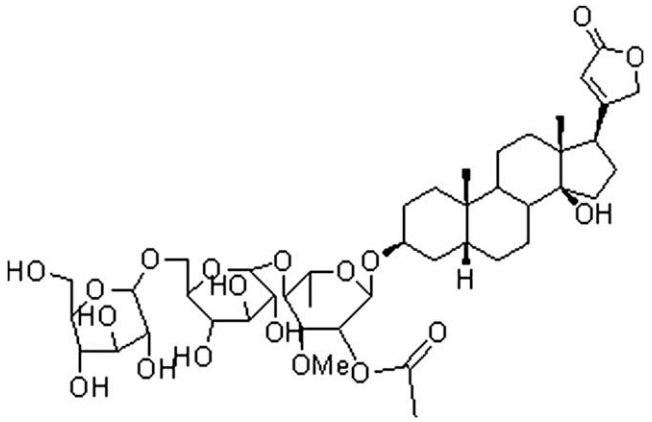

Fig. 1. Chemical structure of GHSC-74.

death via apoptosis or necrosis (Orrenius, 2004; Parekh and Putney, 2005; Rizzuto and Pozzan, 2006). It has also been suggested that apoptosis can be induced in response to alterations in intracellular Ca^{2+} compartmentalization and enhanced mitochondrial Ca^{2+} accumulation (Nutt et al., 2002; Orrenius, 2004). Nutt et al. (2002) and Kirichok et al. (2004) found that the mitochondrial uniporter, a Ca^{2+}-selective ion channel present on the outer mitochondrial membrane, mediated rapid mitochondrial uptake of the Ca^{2+} following release from ER store. In addition, activation of the uniporter, together with a rise in mitochondrial Ca^{2+}, stimulated generation of reactive oxygen species (ROS) and free fatty acids, thus promoting opening of the permeability transition pore (PTP) (Scorrano et al., 2001; Starkov et al., 2004). Opening of the PTP caused dissipation of the mitochondrial membrane potential and eventually the release of Ca^{2+}. However, under certain circumstances, mitochondrial Ca^{2+} accumulation acted as a trigger for release of pro-apoptotic molecules from the mitochondria, leading to execution of the cells (Hajnoczky and Hoek, 2007). *In vivo* and *in vitro* studies of Murphy et al. (1996) showed that Bcl-2 regulates intracellular Ca^{2+} levels and prevents the loss of mitochondrial membrane potential induced by pro-apoptotic stimuli.

The aim of our investigation was to elucidate molecular mechanisms of Ca^{2+}-mediated mitochondrial pathway in GHSC-74-induced HepG2 cell apoptosis.

2. Materials and methods

2.1. Reagents

Reagents used in the present study included Minimal essential medium (MEM), RPMI 1640 medium, Dulbeccco's modified Eagle's medium (DMEM), fetal bovine serum (FBS), newborn calf serum (NCS), penicillin, streptomycin, trypsin-EDTA (GIBCO Laboratories, Grand Island, USA); dimethylsulfoxide (DMSO), 3-(4,5-dimethylthiazol-2-yl)-2,5-diphenylterazolium bromide (MTT), ethylene glycol-bis-(2-aminoethylether)-*N*,*N*,*N*′,*N*′-tetraacetic acid (EGTA), Hoechst 33342, propidium iodide (PI), annexin-V-FITC apoptosis detection kit (Sigma Chemical Co., St. Louis, USA); the mitochondrial membrane potential probe 5,5′,6,6′-tetrachloro-1,1′3,3′-tetraethyl-benzimidazoylcarbocyanine iodide (JC-1) (Invitrogen Molecular Probes, Eugene, USA); Ca^{2+} dye Fluo-3/AM (Calbiochem, Bad Soden, Germany); 1,2-bis(2-aminophenoxy)-ethane-*N*,*N*,*N*′,*N*′-tetraacetic acid (BAPTA)-AM (Dojindo, Kumamoto, Japan); and anti-Bcl-2 andanti-β-actin (Santa Cruz Biotechnology, Santa Cruz, USA). All other chemicals were of analytical grade.

2.2. Test compound

GHSC-74 (purity $\geq$ 95% by ^{1}H nuclear magnetic resonance (NMR) spectroscopy and liquid chromatography–mass spectrum (LC–MS)) was purified by Shanghai Institute of Materia Medica, the Chinese Academy of Sciences according to the previously described method (Abe and Yamauchi, 1977). Briefly, fresh seeds (1.3 kg dry weight) of *C .manghas* L. were cut into pieces and extracted exhaustively with MeOH (3 × 15 L). The MeOH extract was concentrated *in vacuo* to give a residue, which was dissolved in H_2O (1000 ml) and the solution was partitioned consecutively between H_2O and petroleum ether, H_2O and EtOAc, H_2O and *n*-BuOH. The *n*-BuOH extract (62 g) was separated by column chromatography (CC) on silica gel (100–200 mesh). The column was eluted with a gradient of chloroform–MeOH (9:1–0:100) to give six fractions (Fr.1–Fr.6) on the basis of TLC checking. Fraction 1 (9.0 g) was further purified by CC on silica gel (100–200 mesh) and eluted with a gradient of chloroform–MeOH (98:2–9:1), followed by Sephadex LH-20 (chloroform/MeOH 1:1) to give GHSC-77 (4.5 mg) and GHSC-73 (185 mg).

2.3. Cell culture and drug preparation

Human hepatocellular carcinoma (HCC) cell line HepG2, Chang human liver cells and Swiss albino 3T3 fibroblasts were purchased from the cell bank of Shanghai Institute of Cell Biology (Shanghai, China). HepG2 cells were maintained in MEM containing 10% heat-inactivated FBS, and 100 U/ml penicillin plus 100 μg/ml streptomycin. Chang human liver cells were maintained in RPMI 1640 containing 10% heat-inactivated NCS, and 100 U/ml penicillin plus 100 μg/ml streptomycin. Swiss albino 3T3 fibroblasts were maintained in DMEM containing 10% heat-inactivated FBS, and 100 U/ml penicillin plus 100 μg/ml streptomycin. Cells were grown in a 37 °C incubator supplied with 95% air and 5% CO_2. After growing to 60–80% confluency, cells were trypsinized with 0.25% trypsin-EDTA, counted, and placed at the desired density for treatment. GHSC-74 was dissolved in DMSO and further diluted in PBS. The final DMSO concentration was 0.1%, which did not affect cell function and the assay systems.

2.4. Cell proliferation assay

The effect of GHSC-74 on viability of HepG2 cells, Chang human liver cells and Swiss albino 3T3 fibroblasts was

determined with the 3-(4,5-dimethylthiazol-2-yl)-2,5-diphenyltetrazolium bromide (MTT) assay (Mosmann, 1983). Cells were plated at 1×10^4 cells/well in 100 μl complete culture medium and treated with various concentrations of GHSC-74 in 96-well microtiter plates. Each concentration of GHSC-74 (0–40 μM) was repeated in 10 wells. Cell viability was determined 24, 48 and 72 h after incubation at 37 °C in a humidified incubator. MTT (5 mg/ml in PBS) was added to each well and incubated for 4 h. The plate was centrifuged at 1800 rpm for 5 min at 4 °C and the supernatant aspirated from the wells. After careful removal of the medium, 200 μl DMSO was added to each well and shaken well. Absorbance (*A*) was recorded on a microplate reader (Model 550; Bio-Rad, USA) at 550 nm. Cell viability was calculated based on the following formula: cell viability (%) = (average A_{550nm} of treated group/average A_{550nm} of control group) × 100%. The inhibitory effect of GHSC-74 on cell growth was assessed as percent cell viability, where cells without treatment were considered 100% viable.

2.5. Assessment of cell morphological changes

Cell morphological changes were first observed by light microscopy, and then examined for morphological change by nuclear Hoechst 33342 staining as previously described (Park et al., 2005). Cells were washed with PBS and fixed with 4% paraformaldehyde in PBS for 10 min at room temperature. The fixed cells were washed with PBS, and stained with 4 μg/ml Hoechst 33342 for 20 min at room temperature. The cells were washed twice with PBS and visualized with a fluorescence microscope (Olympus, IX70, Japan).

2.6. Annexin-V-FITC/PI assay of apoptotic cells

Apoptosis was determined by annexin-V-FITC staining and PI labeling, because annexin-V can identify externalization of phosphatidylserine during the progression of apoptosis and, therefore, can detect cells in early stages of apoptosis. To quantify apoptosis, prepared cells were washed twice with cold PBS and resuspended in 500 μl binding buffer (10 mM HEPES/NaOH (pH 7.4), 140 mM NaCl and 2.5 mM $CaCl_2$) at a concentration of 1×10^6 cells/ml. Five microliters annexin-V-FITC and 10 μl PI (1 μg/ml) were then added to these cells, which were analyzed with a FACScalibur flow cytometer (Becton Dickinson) and calculated by CellQuest software. Early apoptotic cells were positive for annexin-V and negative for PI, while late apoptotic dead cells displayed both high annexin-V and PI labeling.

2.7. Western blot analysis

Cells were scraped from the culture, washed twice with PBS, and then suspended in 30 μl Western blot lysis buffer containing 50 mM Tris–HCl (pH 7.5), 250 mM NaCl, 1 mM EDTA, 1 mM EGTA, 1 mM NaF, 1 mM phenylmethylsulfonyl fluoride, 1 mM DTT, 20 μg/ml leupeptin, 20 μg/ml aprotinin, 0.1% Trion X-100, and 1% SDS at 0–4 °C for 15 min. After centrifugation at 12,000 × *g* for 5 min at 4 °C, the supernatant was collected, and the protein concentration was determined using bicinchoninic acid (BCA) protein assay (Beyotime Biotechnology, Haimen, China). Equal amounts (50 μg protein) of lysate were subjected to a 12% SDS-PAGE. After electrophoresis, protein blots were transferred to a nitrocellulose membrane using an electro-blotting apparatus (Bio-Rad). The membrane was blocked with 5% nonfat milk in TBST solution, and incubated overnight with the corresponding primary antibodies in the blocking solution at 4 °C. After three washes with TBST solution, the membrane was incubated at room temperature for 1 h, with horseradish peroxidase-conjugated secondary antibody diluted with TBST solution (1:3000). The signals of detected proteins were visualized by an enhanced chemiluminescence reaction (ECL) system (Amersham, ECL kits).

2.8. Measurement of cytosolic [Ca^{2+}]

Cytosolic [Ca^{2+}] was measured by using Fluo-3/AM, a fluorescent dye, which is cleaved and trapped inside cells (Suzuki et al., 1996). Cells were plated in a 6-well plate at a density of 5×10^5 cells/well, as described above. After exposure to GHSC-74 (4 μM) for the designated periods of time, cells were incubated with 8 μM Fluo-3/AM for 45 min at 37 °C in dark, washed twice with PBS, incubated for another 20 min at 37 °C in HEPES buffered Ringer's medium (120 mM NaCl, 5.4 mM KCl, 0.8 mM $MgSO_4$, 1.0 mM $CaCl_2$,11 mM glucose, 20 μM HEPES and 0.2%BSA at pH 7.4), washed again with the same buffer, and finally suspended in 500 μl PBS. Ca^{2+}-dependent fluorescence intensity was measured by flow cytometry on a fluorescence-activated cell sorter (FACSCalibur; Becton Dickinson) in the fluorescence channel FL-1 with excitation at 488 nm and emission at 530 nm.

2.9. Mitochondrial membrane potential assay

The mitochondrial membrane potential was determined quantitatively by flow cytometry using the fluorescent lipophilic cationic probe JC-1 (the probe 5,5′,6,6′-tetrachloro-1,1′,3,3′-tetraethyl-benzimidazolcarbocyanine iodide) Detection Kit following the manufacturer's instructions. JC-1 was selectively concentrated or accumulated within intact mitochondria to form multimer J-aggregates emitting fluorescence light at 590 nm. The monomeric form emits light at 527 nm after excitation at 490 nm. Thus the color of the dye changes from red to green depending on the mitochondrial membrane potential, and can be analyzed by FACS with green fluorescence in channel 1(FL1). Briefly, HepG2 cells were treated with GHSC-74 (4 μM) for 24 h and 48 h, harvested, and washed with PBS. A total of 1×10^6 cells were incubated in 1 ml PBS containing 10 μg JC-1 for 15 min at 37 °C in the dark. Stained cells were washed, resuspended in 500 μl PBS, and analyzed on a flow cytometer (FACScalibur; Becton Dickinson).

2.10. Statistical analysis

All data are presented as mean ± S.D. All experiments were done at least three times, and three or more independent

observations were made on each occasion. Statistically significant values were compared using Student's *t*-test for single comparison and *p*-values <0.05 were considered statistically significant.

3. Results

3.1. Cytotoxic activity of GHSC-74

One tumorigenic human cell line HepG2 and two normal cell lines (Chang human liver cells and Swiss albino 3T3 fibroblasts) were chosen to determine cytotoxic activity of GHSC-74. A typical dose- and time-dependent inhibitory effect on cell growth was observed in HepG2 cells with an IC_{50} (median growth inhibitory concentration value) of ~0.5 μM following treatment with GHSC-74 for 48 h (Fig. 2A). However, the doses (0–80 μM) of GHSC-74 did not significantly decrease the viability of Chang human liver cells and Swiss albino 3T3 fibroblasts (Fig. 2B). The higher dose (80 μM) of GHSC-74 reduced the viability of Chang human liver cells and Swiss albino 3T3 fibroblasts by ~7 and 30%, respectively. These results demonstrated that GHSC-74 had a significant inhibitory effect on proliferation of HepG2 cells without significantly reducing the viability of normal cells.

3.2. GHSC-74 induces apoptosis in HepG2 cells

Hoechst staining was performed to determine whether the inhibitory effect of GHSC-74 on cell growth was associated with the induction of apoptosis. Fig. 3A shows that the nuclear structure of control cells was intact, while condensed chromatin and formation of apoptotic bodies were seen in the nuclei of HepG2 cells cultured with 4 μM GHSC-74 for 48 h, where the characteristic morphological change of apoptosis was seen. However, the nuclear structure of Swiss albino 3T3 fibroblasts with or without treatment of GHSC-74 remained intact (Fig. 3B).

To further confirm that it was GHSC-74 that induced cell apoptosis, HepG2 cells were stained with annexin-V-FITC and PI, and then analyzed by flow cytometry. The proportion of annexin-V-staining cells in GHSC-74-treated HepG2 cells increased markedly in a time- and dose-dependent manner (Fig. 3C,D). There was a marked and dose-dependent increase in the number of early apoptotic cells, ranging from $1.17 \pm 0.12\%$ to $14.26 \pm 2.34\%$ at 48 h and from $1.94 \pm 0.43\%$ to $33.40 \pm 2.72\%$ at 72 h after incubation with different concentrations (0–8 μM) of GHSC-74. HepG2 cells with a small amount of necrosis (annexin-V-negative and PI positive proportion of cells) were observed.

The above results suggested that the cytotoxic effects observed in response to GHSC-74 were associated with induction of apoptotic cell death.

3.3. $[Ca^{2+}]_i$ is involved in GHSC-74-induced HepG2 cell apoptosis

An abnormal elevation of cytosolic Ca^{2+} is one of the major features of apoptosis (Carafoli and Molinari, 1998; McConkey and Orrenius, 1996, 1997). To examine whether GHSC-74-induced apoptosis was associated with increased cytosolic Ca^{2+}, we evaluated the intensity of cytosolic Fluo-3 fluorescence, an indicator of cytosolic Ca^{2+} in HepG2 cells treated with or without GHSC-74. Following treatment with GHSC-74 (4 μM) for 48 h, cytosolic Ca^{2+} was 4.8 times the control; GHSC-74 (4 μM) caused a transient and sustained elevation of cytosolic Ca^{2+} compared to the control (Fig. 4A).

To identify the origin of cytosolic Ca^{2+} increased, cells were pre-incubated with BAPTA-AM (5 μM) to chelate the cytosolic Ca^{2+}, while EGTA (1 mM) in the culture medium was used to chelate the extracellular Ca^{2+}, knowing that cytosolic Ca^{2+} elevation is either due to Ca^{2+} influx from the external medium or due to Ca^{2+} released from internal stores. BAPTA-AM partly suppressed GHSC-74-induced cell death (Fig. 4B). In contrast, EGTA exhibited little effect as compared to BAPTA-AM (Fig. 4C), suggesting that increased cytosolic Ca^{2+} in HepG2 cells was largely attributed to redistribution of intracellular Ca^{2+}. Fig. 4D,E also shows that BAPTA-AM partly blocked mitochondrial membrane

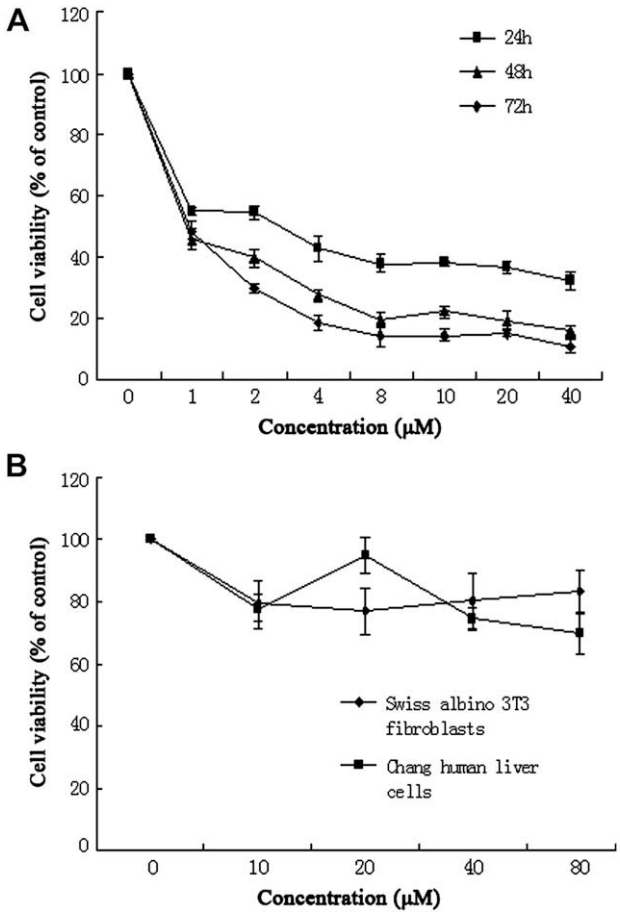

Fig. 2. Effect of GHSC-74 on cytotoxicity. (A) HepG2 cells were treated with different concentrations (0–40 μM) of GHSC-74 for 24, 48 and 72 h. (B) Chang human liver cells and Swiss albino 3T3 fibroblasts were treated with different concentrations (0–80 μM) of GHSC-74 for 48 h. Cell proliferation was determined by MTT assay, as previously described. Values are represented as the percentage of viable cells; vehicle-treated cells were considered as 100% viable. The data represent mean percentages of viable cells ± SD of three independent experiments.

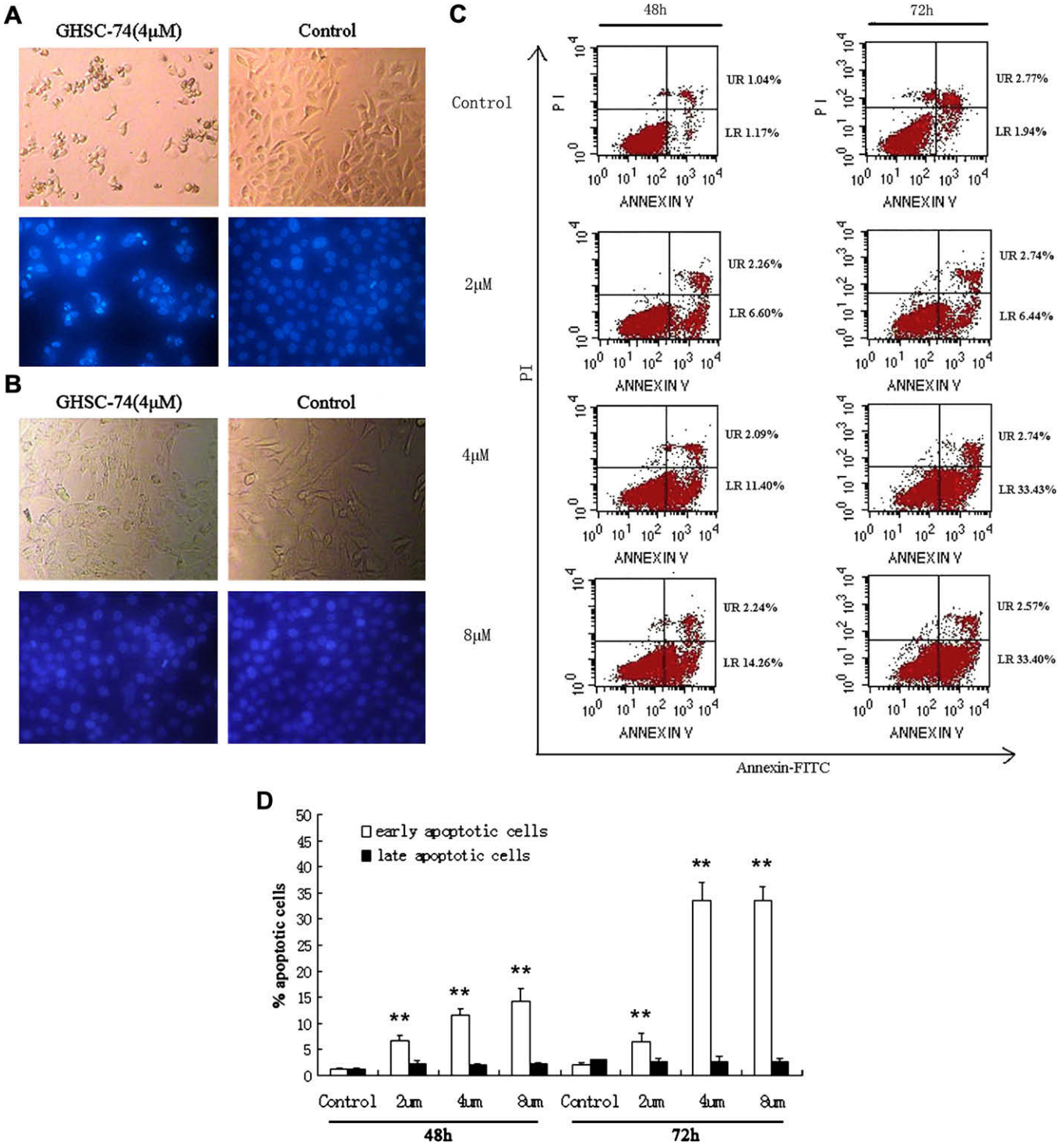

Fig. 3. GHSC-74-induced apoptosis in HepG2 cells. (A) Morphological change of HepG2 cells after treatment with GHSC-74 (4 μM) for 48 h. Cells treated with or without GHSC-74 were observed by light microscopy (magnification 250×). Characteristic apoptosis (nuclear shrinkage, presence of apoptotic bodies and membrane blebbing) was seen on fluorescence micrographs of GHSC-74-treated cells stained with Hoechst 33342 (magnification 200×), while the nuclei of control cells stained with Hoechst 33342 looked normal on fluorescence micrographs (magnification 200×). Data are representative of 3 independent experiments. (B) Morphological change of Swiss albino 3T3 fibroblasts after treatment with GHSC-74 (4 μM) for 48 h. The nuclei of cells treated with or without GHSC-74 looked normal. Data are representative of three independent experiments. (C) Detection of GHSC-74-induced apoptosis and necrosis with annexin-V-FITC and PI staining. Exponentially growing cells were treated with the designated concentrations of GHSC-74 for 48 and 72 h. Cells with annexin-V and PI staining were measured by flow cytometry. (D) A graph showing the percentage of early apoptotic cells and late apoptotic cells from C. The data represent the mean ± S.D. of three independent experiments. Asterisks indicate significant difference from control (**$p < 0.01$).

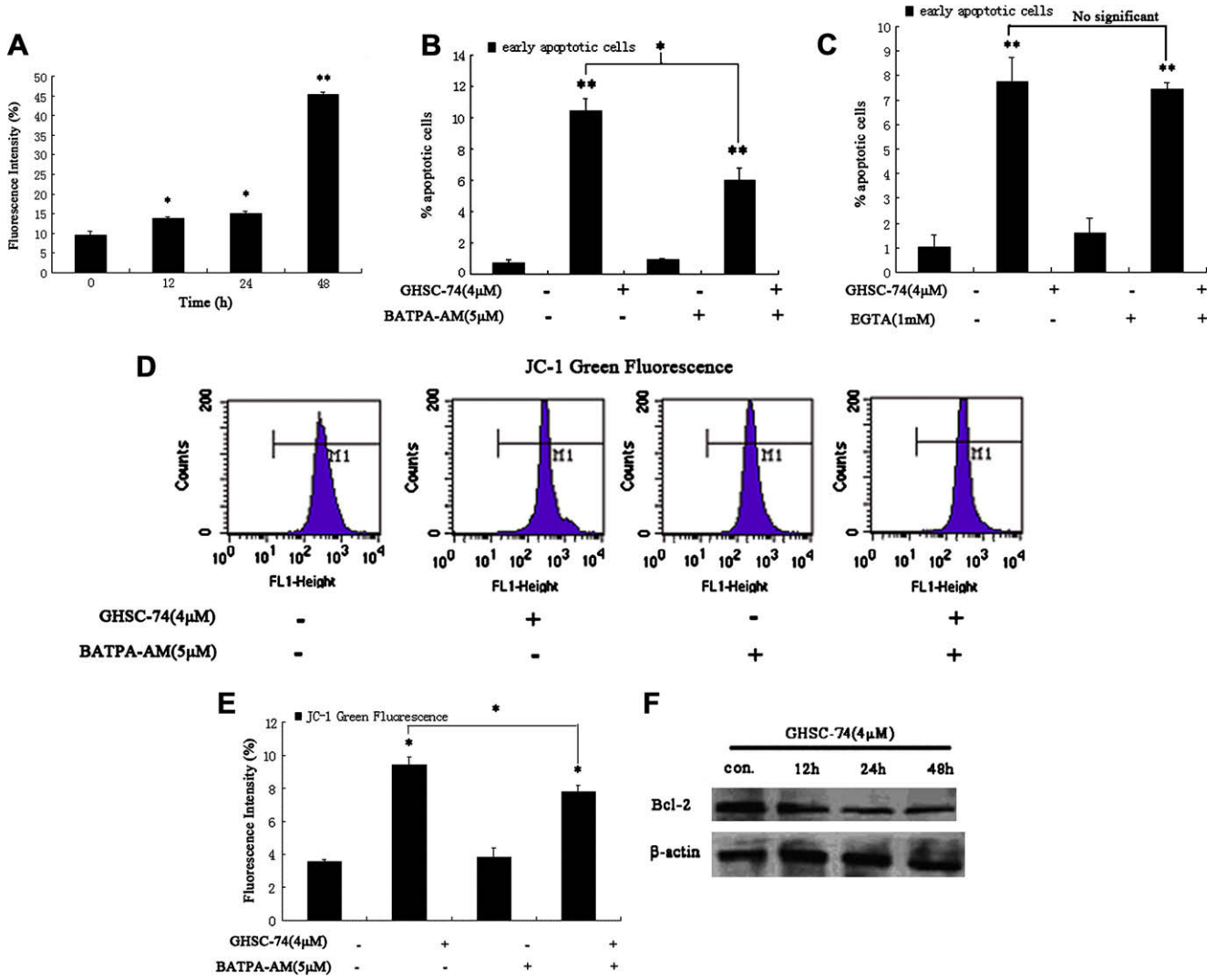

Fig. 4. $[Ca^{2+}]_i$ was involved in HepG2 cell apoptosis induced by GHSC-74. (A) Time-course effect of GHSC-74 (4 μM) on cytosolic Ca^{2+} in HepG2 cells after treatment for 0, 12, 24 and 48 h. Cells loaded with Fluo-3/AM (8 μM) were measured by flow cytometry. (B) and (C) Cells were pre-incubated with BAPTA-AM (5 μM) or EGTA (1 mM) for 30 min and further incubated with 4 μM GHSC-74 for 48 h. Apoptosis was analyzed by FACS using double staining with FITC-labeled annexin-V and PI. (D) and (E) After pretreatment with 5 μM BATPA-AM for 30 min, cells were treated with GHSC-74 for 48 h and incubated with JC-1 prior to flow cytometric analysis as described previously. Each experiment was performed in triplicate and the data represent the mean ± S.D. $*p < 0.05$, $**p < 0.01$, compared with control. (F) Cells were treated with 4 μM GHSC-74, and 50 μg protein was separated on a 12% SDS-PAGE gel. β-Actin was included as an internal standard to normalize loadings.

depolarization in HepG2 cells treated by GHSC-74, indicating that elevation of $[Ca^{2+}]i$ was partly responsible for the collapse of $\Delta\Psi m$ in GHSC-74-treated HepG2 cells.

Proteins of the Bcl-2 family are critical determinants of the cellular threshold for apoptosis (Yang et al., 1997). GHSC-74 time-dependently decreased the protein abundance of Bcl-2 in HepG2 cells as early as 12 h after treatment (Fig. 4F).

4. Discussion

Many efforts have been made to search for compounds that can influence apoptosis and understand mechanisms of their actions. In recent years, more knowledge has been obtained about how cardiac glycosides induce cell death in human cancers.

Recently, several lines of evidence have shown that intracellular Ca^{2+} plays a critical role in apoptosis, probably through the direct activation of caspases or collapse of $\Delta\Psi m$ (Assaf et al., 2004). In addition, two hypotheses have been proposed to explain the involvement of Ca^{2+} in the apoptotic process. The first is that the depletion of intracellular stores (such as endoplasmic reticulum) and possibly the influx of extracellular Ca^{2+} promote an increase of cytosolic Ca^{2+} that acts as a signal for apoptosis. The second hypothesis is the emptying of intracellular Ca^{2+} stores that trigger apoptosis, perhaps by disrupting the intracellular architecture, thus allowing key elements of the effector machinery (e.g. DNase 1) to gain access to their substrates (McConkey and Orrenius, 1997). Mammalian cells normally maintain $[Ca^{2+}]i$ at ~100 nM, which is 10,000-fold lower than extracellular Ca^{2+}, sequestering Ca^{2+} for

intracellular signaling. Two major types of intracellular Ca^{2+} stores exist (Carafoli, 1987): (1) endoplasmic reticulum (ER), which functions as a high-affinity, low-capacity Ca^{2+} pool, and (2) mitochondria, which are low-affinity, high-capacity Ca^{2+} pool. Bcl-2 may prevent cell death by regulating Ca^{2+} flux through ER (Baffy et al., 1993; Distelhorst et al., 1996; Lam et al., 1994) or mitochondria (Murphy et al., 1996). Mitochondria have the capacity to store Ca^{2+} as calcium phosphate and to buffer physiological increases in $[Ca^{2+}]i$ provided the mitochondrial membrane potential is maintained. Mitochondrial accumulate large loads of Ca^{2+} under conditions of rapid and prolonged entry of Ca^{2+} into the cytoplasm, which occurs during treatment with cytotoxic agents such as H_2O_2. Excess Ca^{2+} loads cause mitochondrial respiratory impairment, followed by a decrease in membrane potential and Ca^{2+} efflux from the mitochondria (Murphy et al., 1996).

GHSC-74 caused a transient and sustained elevation of cytosolic Ca^{2+} in HepG2 cells (Fig. 4A). BAPTA-AM partly blocked cell apoptosis and death induced by GHSC-74 (Fig. 4B) and suppressed the $\Delta\Psi m$ decrease (Fig. 4D and 4E), both of which imply that HepG2 cell apoptosis was partly controlled by cytosolic Ca^{2+} increase. In contrast to BAPTA-AM, EGTA exhibited little effect on GHSC-74-induced cell apoptosis (Fig. 4C), implying that extracellular Ca^{2+} influx also made little contribution to increased cytosolic Ca^{2+}. We conclude that combinatory cytosolic Ca^{2+} increase in HepG2 cells by the depletion of intracellular stores (such as endoplasmic reticulum) after GHSC-74 treatment triggers cell apoptosis; thus, the second hypothesis and extracellular Ca^{2+} influx could be excluded. Besides, it is noteworthy to mention that BAPTA-AM only partially inhibited GHSC-74-induced cell apoptosis and suppressed the $\Delta\Psi m$ decrease, implying that the Ca^{2+}-dependent mitochondrial pathway is not the only pathway involved in GHSC-74-induced cell apoptosis.

However, GHSC-74 decreased the protein level of Bcl-2 in HepG2 cells (Fig. 4F). Several other reports (Mathai et al., 2005) noted that redistribution of intracellular Ca^{2+} was tightly regulated by Bcl-2 oncogene. Bcl-2 has been demonstrated to act as an ion channel in isolated bilayers (Minn et al., 1997) and display a complex distribution in cells (Lithgow et al., 1994). Co-localization of Bcl-2 with Ca^{2+} pumps and channels on ER and the nuclear membrane has raised the possibility that Bcl-2 may play a role in maintaining Ca^{2+} homeostasis in these compartments. Therefore, whether inhibition of Bcl-2 in GHSC-74-treated HepG2 cells is closely related to redistribution of intracellular $[Ca^{2+}]$ awaits more experiments to elucidate.

In conclusion, GHSC-74 is a potent anti-proliferative to HepG2 cells, and may be a promising chemopreventive or chemotherapeutic agent.

Acknowledgments

This work was supported by National Ocean 863 Project by the Ministry of Science and Technology of the People's Republic of China (# 2006AAD9Z447).

References

Abe F, Yamauchi T. Studies on Cerbera. I. Cardiac glycosides in the seeds, bark, and leaves of *Cerbera manghas* L. Chem Pharm Bull 1977;25:2744–8.

Altamirano J, Li Y, DeSantiago J, Piacentino 3rd V, Houser SR, Bers DM. The inotropic effect of cardioactive glycosides in ventricular myocytes requires Na^+/Ca^{2+} exchanger function. J Physiol 2006;575:845–54.

Assaf H, Azouri H, Pallardy M. Ochratoxin A induces apoptosis in human lymphocytes through down regulation of Bcl-xL. Toxicol Sci 2004;79:335–44.

Baffy G, Miyashita T, Williamson JR, Reed JC. Apoptosis induced by withdrawal of interleukin-3 (IL-3) from an IL-3-dependent hematopoietic cell line is associated with repartitioning of intracellular calcium and is blocked by enforced Bcl-2 oncoprotein production. J Biol Chem 1993;268:6511–9.

Braunwald E. Effects of digitalis on the normal and the failing heart. J Am Coll Cardiol 1985;5:51A–9A.

Carafoli E. Intracellular calcium homeostasis. Annu Rev Biochem 1987;56:395–433.

Carafoli E, Molinari M. Calpain: a protease in search of a function? Biochem Biophys Res Commun 1998;247:193–203.

Distelhorst CW, Lam M, McCormick TS. Bcl-2 inhibits hydrogen peroxide-induced ER Ca^{2+} pool depletion. Oncogene 1996;12:2051–5.

Hajnoczky G, Hoek JB. Cell signaling. Mitochondrial longevity pathways. Science 2007;315:607–9.

Kirichok Y, Krapivinsky G, Clapham DE. The mitochondrial calcium uniporter is a highly selective ion channel. Nature 2004;427:360–4.

Lam M, Dubyak G, Chen L, Nunez G, Miesfeld RL, Distelhorst CW. Evidence that Bcl-2 represses apoptosis by regulating endoplasmic reticulum-associated Ca^{2+} fluxes. Proc Natl Acad Sci USA 1994;91:6569–73.

Lithgow T, van Driel R, Bertram JF, Strasser A. The protein product of the oncogene Bcl-2 is a component of the nuclear envelope, the endoplasmic reticulum, and the outer mitochondrial membrane. Cell Growth Differ 1994;5:411–7.

Mathai JP, Germain M, Shore GC. BH3-only Bik regulates BAX, BAK-dependent release of Ca^{2+} from endoplasmic reticulum stores and mitochondrial apoptosis during stress-induced cell death. J Biol Chem 2005;280:23829–36.

McConkey DJ, Orrenius S. The role of calcium in the regulation of apoptosis. J Leukoc Biol 1996;59:775–83.

McConkey DJ, Orrenius S. The role of calcium in the regulation of apoptosis. Biochem Biophys Res Commun 1997;239:357–66.

Minn AJ, Velez P, Schendel SL, Liang H, Muchmore SW, Fesik SW, et al. Bcl-x(L) forms an ion channel in synthetic lipid membranes. Nature 1997;385:353–7.

Mosmann T. Rapid colorimetric assay for cellular growth and survival: application to proliferation and cytotoxic assays. J Immunol Methods 1983;65:55–63.

Murphy AN, Bredesen DN, Cortopassi G, Wang E, Fiskum G. Bcl-2 potentiates the maximal calcium uptake capacity of neural cell mitochondria. Proc Natl Acad Sci USA 1996;93:9893–8.

Nutt LK, Chandra J, Pataer A, Fang B, Roth JA, Swisher SG, et al. Bax and Bak promote apoptosis by modulating endoplasmic reticular and mitochondrial Ca^{2+} stores. J Biol Chem 2002;277:20301–8.

Orrenius S. Mitochondrial regulation of apoptotic cell death. Toxicol Lett 2004;149:19–23.

Parekh AB, Putney Jr JW. Store-operated calcium channels. Physiol Rev 2005;85:757–810.

Park SY, Cho SJ, Kwon HC, Lee KR, Rhee DK, Pyo S. Caspase-independent cell death by allicin in human epithelial carcinoma cells: involvement of PKA. Cancer Lett 2005;224:123–32.

Poon RT, Fan ST, Lo CM, Ng IO, Liu CL, Lam CM, et al. Improving survival results after resection of hepatocellular carcinoma: a prospective study of 377 patients over 10 years. Ann Surg 2001;234:63–70.

Rizzuto R, Pozzan T. Microdomain of intracellular Ca^{2+}: molecular determinants and functional consequences. Physiol Rev 2006;86:369–408.

Schwartz M. Liver transplantation for hepatocellular carcinoma. Gastroenterology 2004;127:S268–76.

Scorrano L, Penzo D, Petronilli V, Pagano F, Bernardi P. Arachidonic acid causes cell death through the mitochondrial permeability transition.

Implications for tumor necrosis factor-alpha apoptotic signaling. J Biol Chem 2001;276:12035–40.

Starkov AA, Chinopoulos C, Fiskum G. Mitochondrial calcium and oxidative stress as mediators of ischemic brain injury. Cell Calcium 2004;36:257–64.

Steffen F, Manuela FS, Anne-Catherine A, Daniela M, Beatrice Z, Ralph AS. Cardiac glycosides initiate Apo2L/TRAIL-induced apoptosis in non–small cell lung cancer cells by up-regulation of death receptors 4 and 5. Cancer Res 2006;66:5867–74.

Suzuki M, Harada S, Owaribe K, Yaoita H. Intracellular ionic changes induced by bullous pemphigoid IgG subclasses. Autoimmunity 1996;23:181–97.

Wilhelm S, Georgios SB. Endogenous and exogenous cardiac glycosides: their roles in hypertension, salt metabolism, and cell growth. Am J Physiol Cell Physiol 2007;293:C509–36.

Yang J, Liu X, Bhalla K, Kim CN, Ibrado AM, Cai J, et al. Prevention of apoptosis by Bcl-2: release of cytochrome c from mitochondria blocked. Science 1997;275:1129–32.